NUREG/CR-0425
BMI-2005

AEROSOL MEASUREMENTS AND MODELING FOR FAST REACTOR SAFETY

Quarterly Progress Report
January through March, 1978

J.A. Gieseke K.W. Lee
H. Jordan B. Vaishnavi

Battelle — Columbus Laboratories

Prepared for
U.S. Nuclear Regulatory Commission

Available from
National Technical Information Service
Springfield, Virginia 22161
Price: Printed Copy $4.50 ; Microfiche $3.00

The price of this document for requesters outside of the North American Continent can be obtained from the National Technical Information Service.

NUREG/CR-0425
BMI-2005

AEROSOL MEASUREMENTS AND MODELING FOR FAST REACTOR SAFETY

Quarterly Progress Report
January through March, 1978

J.A. Gieseke
H. Jordan
K.W. Lee
B. Vaishnavi

Manuscript Completed: September 1978
Date Published: October 1978

Battelle — Columbus Laboratories
505 King Avenue
Columbus, OH 43201

Prepared for the
Division of Reactor Safety Research
Office of Nuclear Regulatory Research
U.S. Nuclear Regulatory Commission
Under Contract No. NRC-04-76-293-07

TABLE OF CONTENTS

List of Tables

List of Figures

AEROSOL MEASUREMENTS AND MODELING FOR FAST REACTOR SAFETY

QUARTERLY PROGRESS REPORT FOR JANUARY THROUGH MARCH, 1978

J. A. Gieseke
H. Jordan
K. W. Lee
B. Vaishnavi

INTRODUCTION

Technical progress during this quarter was made on the comparison of the HAARM-3 computer code with aerosol measurements, experimental measurements of uranium oxide aerosol characteristics, determinations of humidity effects on sodium aerosol formation, and development of the reference code. In addition, a mid-year review was presented to NRC staff on February 16, 1978. Technical progress on each of the above topics is discussed in this report.

CODE COMPARISON FOR THE CASSANDRE GEOMETRY

Efforts to compare HAARM-3 code calculations with available experimental data have been continued and are described here. The experimental results used are those of the CASSANDRE tests conducted by the Commissariat à l'Energie Atomique of France. The results of CASSANDRE tests have already been compared with the calculations using the PARDISEKO-III and HAARM-2 codes[1]. These experimental results have now been compared with HAARM-3 predictions and the results are described briefly here.

The CASSANDRE tests were conducted in a 400 m^3 containment of nearly cubical configuration. The aerosol used is sodium oxide which was generated by a pool fire. A total of six tests have been reported with the amount of sodium burned ranging from 14 to 300 kg and the source duration time ranging from 40 to 260 minutes. Table 1 shows the experimental conditions of each test.

TABLE 1. SOURCE DATA FOR CASSANDRE EXPERIMENTS

Test No.	Sodium Mass Burned, kg	Source Duration, min.
CASSANDRE:		
02	14	40
03	42	80
04	82	130
05	115	180
07	300	260
08	301	120

It was found that the geometric number mean diameter of the aerosol size distribution ranged from 0.12 to 0.51 μm. The geometric standard deviation of the aerosol distribution was measured to be between 1.5 and 2.5. In measuring the above size distribution parameters, electromicroscopy of samples taken by thermal precipitation was used.

Figures 1 through 6 compare the experimental and HAARM-3 calculated results for the six CASSANDRE tests. The input data used for these calculations were those reported to have been used for the comparisons of the data with HAARM-2 and PARDISEKO-III calculations[1]. These data are shown in Table 2. By making use of these input data, the HAARM-3 calculation results can be directly compared with results of the calculations with the HAARM-2 and PARDISEKO-III codes in addition to the experimental data.

The size distribution parameters of source aerosol based on the measured data reported to have been used as the inputs, i.e., the mass median particle size and geometric standard deviation are given in Table 2. Based on these and the amount of sodium oxidized, the source rate was calculated assuming a constant source release. However, as seen from Table 2, the source particle sizes are widely spread among the different tests

TABLE 2. LIST OF INPUT DATA USED IN THE HAARM-3 CALCULATIONS

Input	Test No.							
	02	03	04	05			07	08
Source Rate, particles/sec-cc	1.085×10^5	3.63×10^2	1.15×10^4	9.267×10^2			2.736×10^4	2.394×10^4
Geometric Std. Dev.	2.5	2.16	2.11	2.28	2.0	2.0	1.86	2.5
R_{50}, μm	0.196	3.0	0.985	2.762	0.5	0.5	0.698	1.738
Source Duration Time, min.	40	80	130	180	180	60	260	120
Vessel Temp., K	300	300	300	300	300	300	300	300
Temp. Gradient, K/cm	300	300	300	300	300	300	300	300

ranging from 0.196 to 3.01 μm in mass median radius. These values can be compared to 0.5 μm which was previously used in HAARM-3 calculations of comparisons with other data. Particularly, the mass median source aerosol radius of 3.0 μm and 2.762 μm used in the CASSANDRE Tests 03 and 05, respectively, appear to be too high. As a check for Test 05, calculations were also made using 0.5 μm for the mass median radius as indicated in Table 2. Vessel temperature and pressure were taken as 300 K and 1 atmosphere for all runs since experimental data on these parameters were not available. These values are in agreement with the conditions normally found in other experiments. The temperature gradient at the wall of 300 K/cm was again used as in the original report[1]. However, it should be noted that this value seems to be higher than those found in other experiments such as the NSPP tests[2].

In general, it is seen from Figures 1 through 6, that the HAARM-3 calculations predict the measured aerosol concentration closely. However, it is also seen that in certain instances, the HAARM-3 calculations underpredict the aerosol concentration slightly. For example, Figure 6 shows that measured aerosol concentrations at the time between about 150 and 350 minutes remain higher than the predicted concentrations. A possible explanation for this is as follows. The measured mass median particle radius of 1.738 μm seems to be too high compared to values of 0.5 μm measured by other experimenters[3]. It is well known that the sodium particles coagulate very rapidly upon being released. For this reason, accurate measurement of the primary particle size of the sodium aerosol during a large-scale sodium fire is often difficult and the measured sizes tend to be somewhat larger than the true initial sizes. If these large values are used in the HAARM-3 calculations, the settling rate due to gravity is enhanced resulting in predicted aerosol concentrations being too low. Similarly, a high value of the geometric standard deviation tends to make the HAARM-3 code predict a reduced aerosol concentration. Compared with a value of 1.5 or 2.0, which was used for other experimental comparisons, the present value of 2.5 for the standard deviation used in Figure 6 also seems to be too high.

Another important consideration for comparisons between experimental data and predictions is to use the time-varying sodium source rate which very closely matches those observed in the tests. Since the information on the actual time-varying source rate was not readily available for the comparisons, the source rates have been calculated under the assumption of constant burning. More specifically, these were calculated by dividing the total amount of sodium oxide by the source cutoff time. These assumed rates are listed in Table 2. Some results of the actual tests indicate, however, that a substantial amount of sodium is burned rapidly early during the fire as can be observed in the measured concentration data appearing in Figure 2. The measured aerosol concentration begins to decrease as early as at the time of about 30 minutes, while the final source cutoff time is shown to be as late as 80 minutes. A similar observation can also be made in Figure 5. It is considered that those mismatches and uncertainties in the source rate also contributed to make the present comparisons less satisfactory.

For summary, the two following remarks may be made:

(1) When a set of comparable input data are used in calculations, it was shown that the HAARM-3 code predicts aerosol concentrations less conservatively than either the HAARM-2 or the PARDISEKO-III codes.

(2) Although they did not lead to large underestimates of airborne concentrations, selections of aerosol properties believed to be in error did lead to some underestimation of airborne concentrations when used in the HAARM-3 code. These results point out the importance of making accurate measurements of the experimental conditions and in particular, of aerosol properties during experimental investigations.

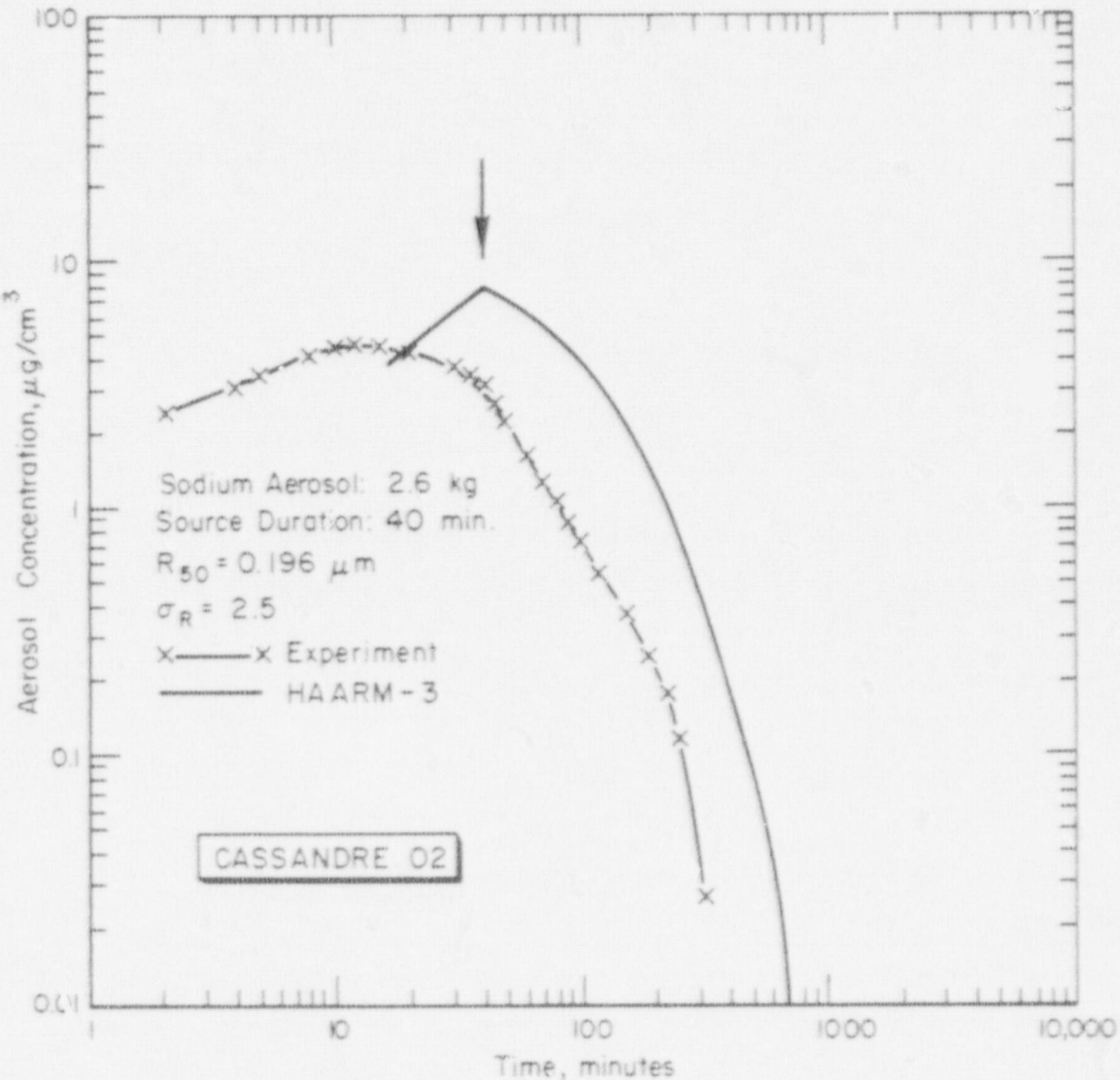

FIGURE 1. COMPARISON OF HAARM-3 CALCULATIONS WITH EXPERIMENTAL DATA -- CASSANDRE TEST 02

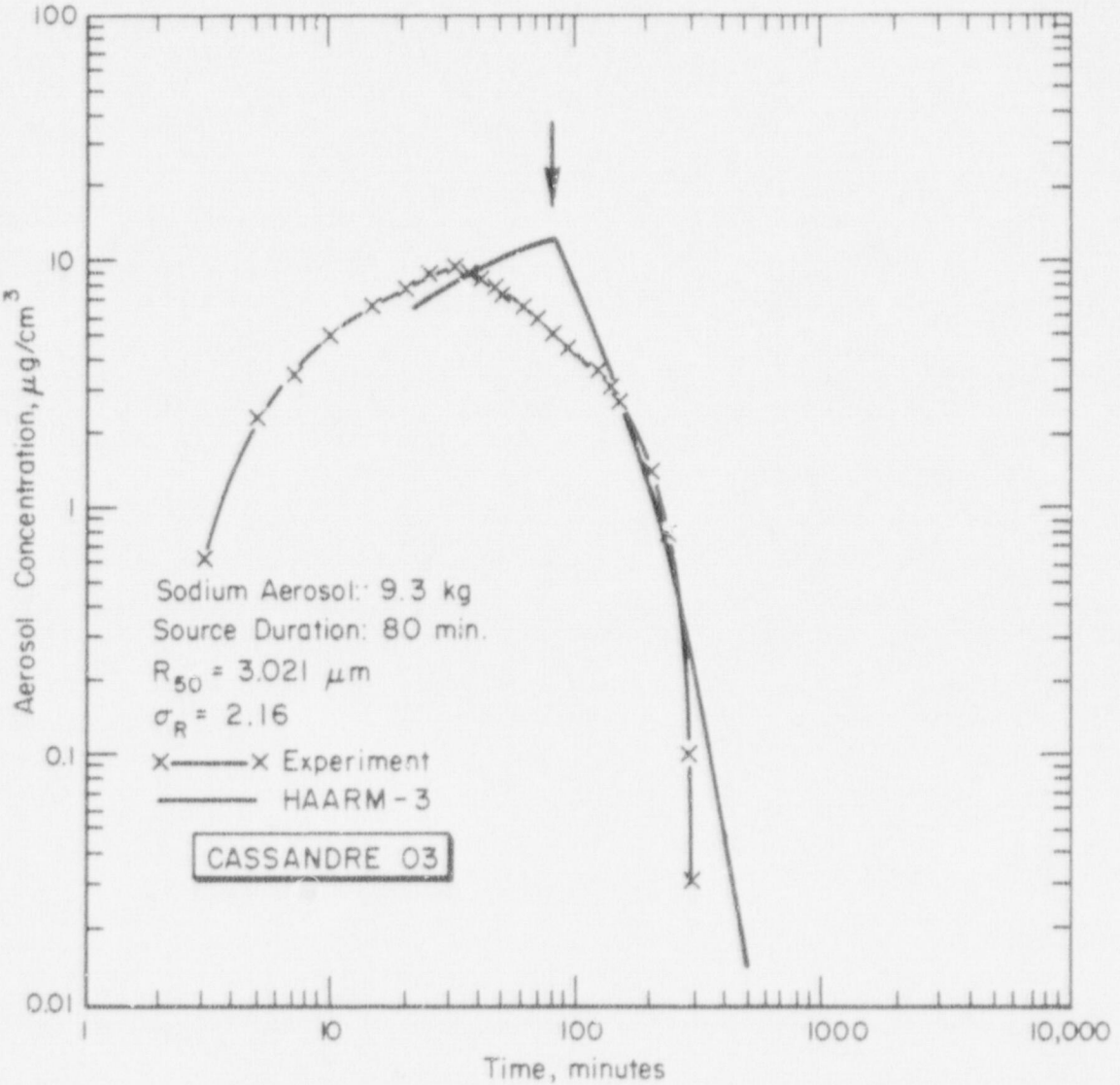

FIGURE 2. COMPARISON OF HAARM-3 CALCULATIONS WITH EXPERIMENTAL DATA -- CASSANDRE TEST 03

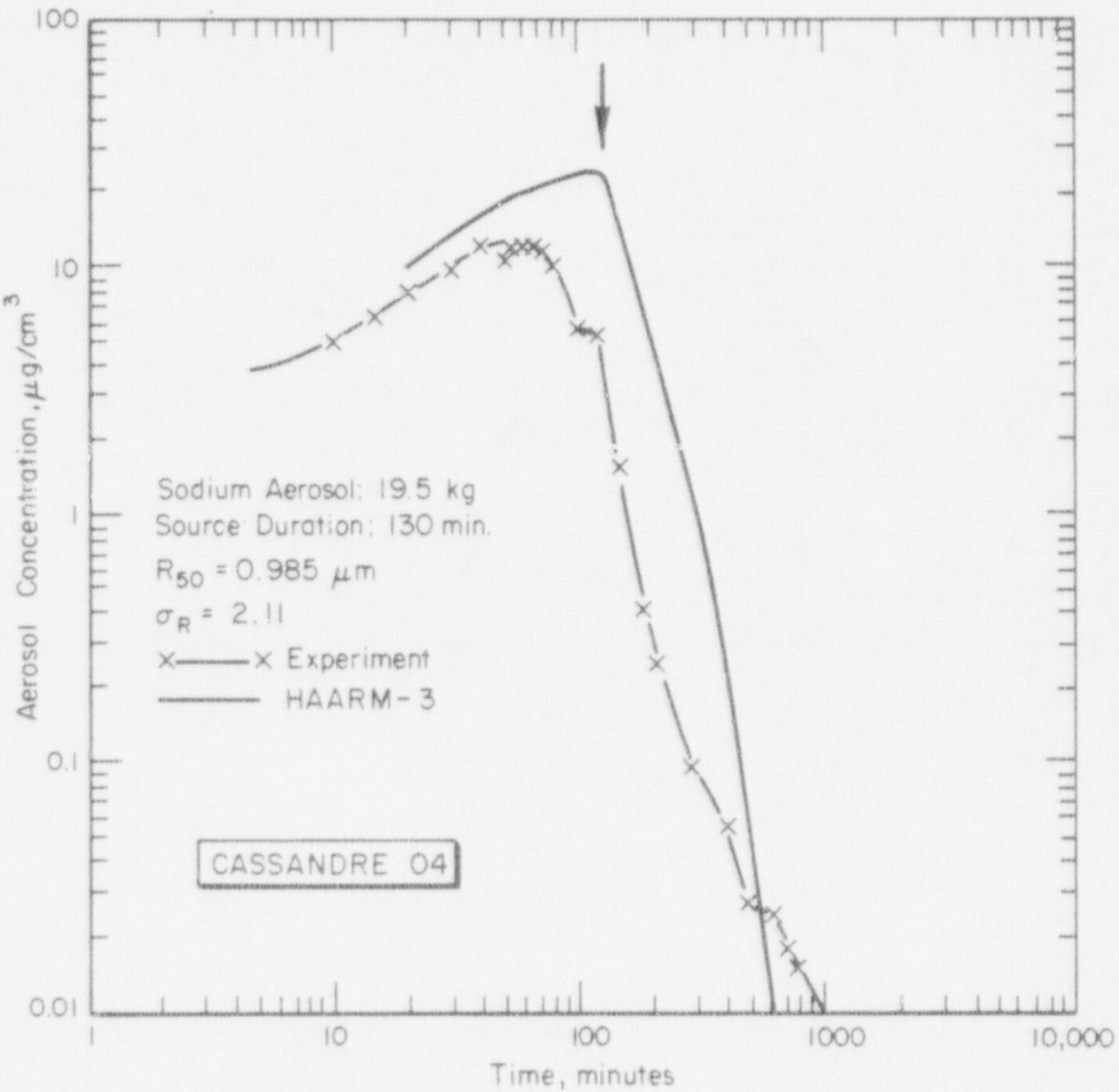

FIGURE 3. COMPARISON OF HAARM-3 CALCULATIONS WITH EXPERIMENTAL DATA -- CASSANDRE TEST 04

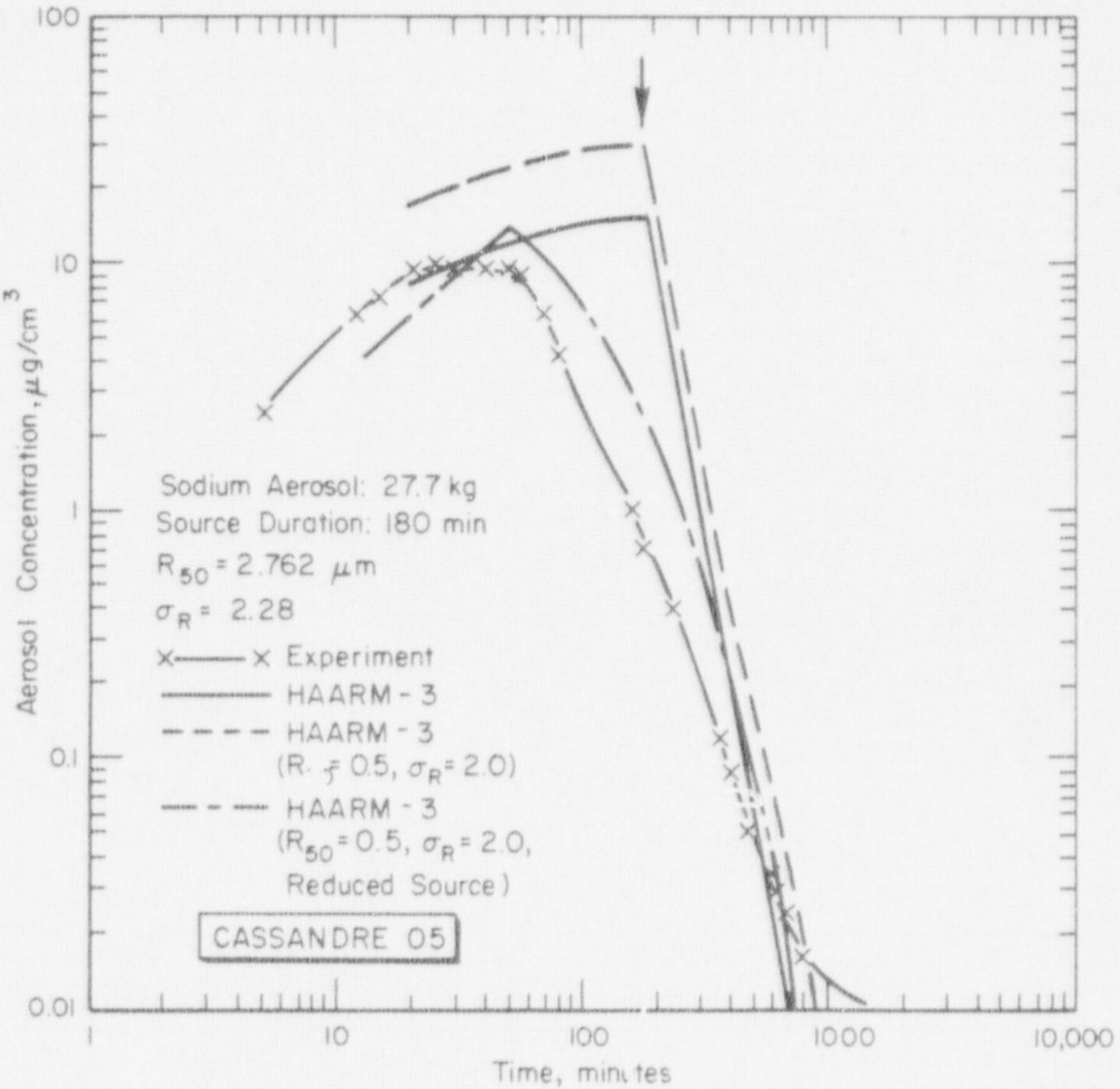

FIGURE 4. COMPARISON OF HAARM-3 CALCULATIONS WITH EXPERIMENTAL DATA -- CASSANDRE TEST 05

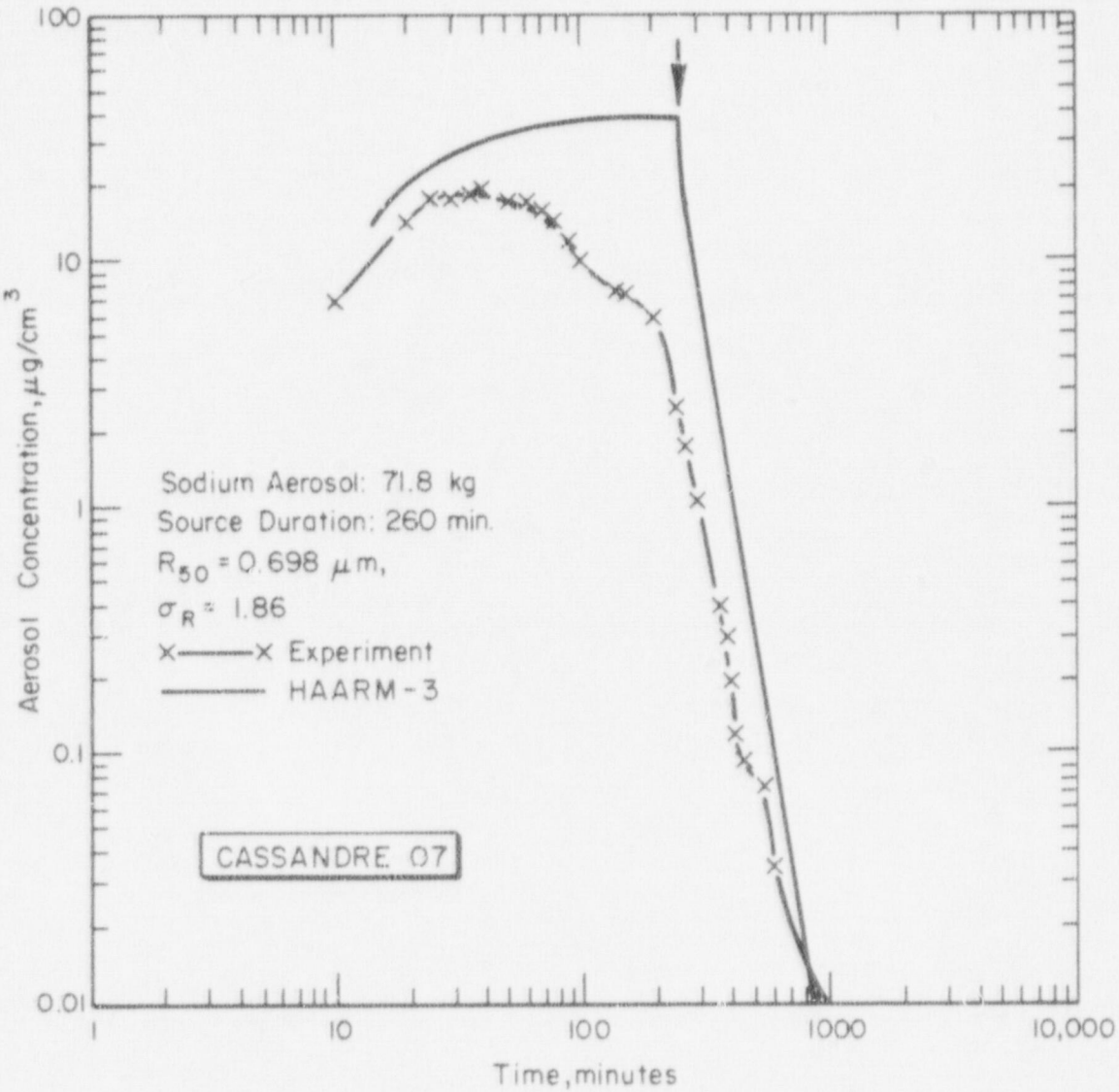

FIGURE 5. COMPARISON OF HAARM-3 CALCULATIONS WITH EXPERIMENTAL DATA -- CASSANDRE TEST 07

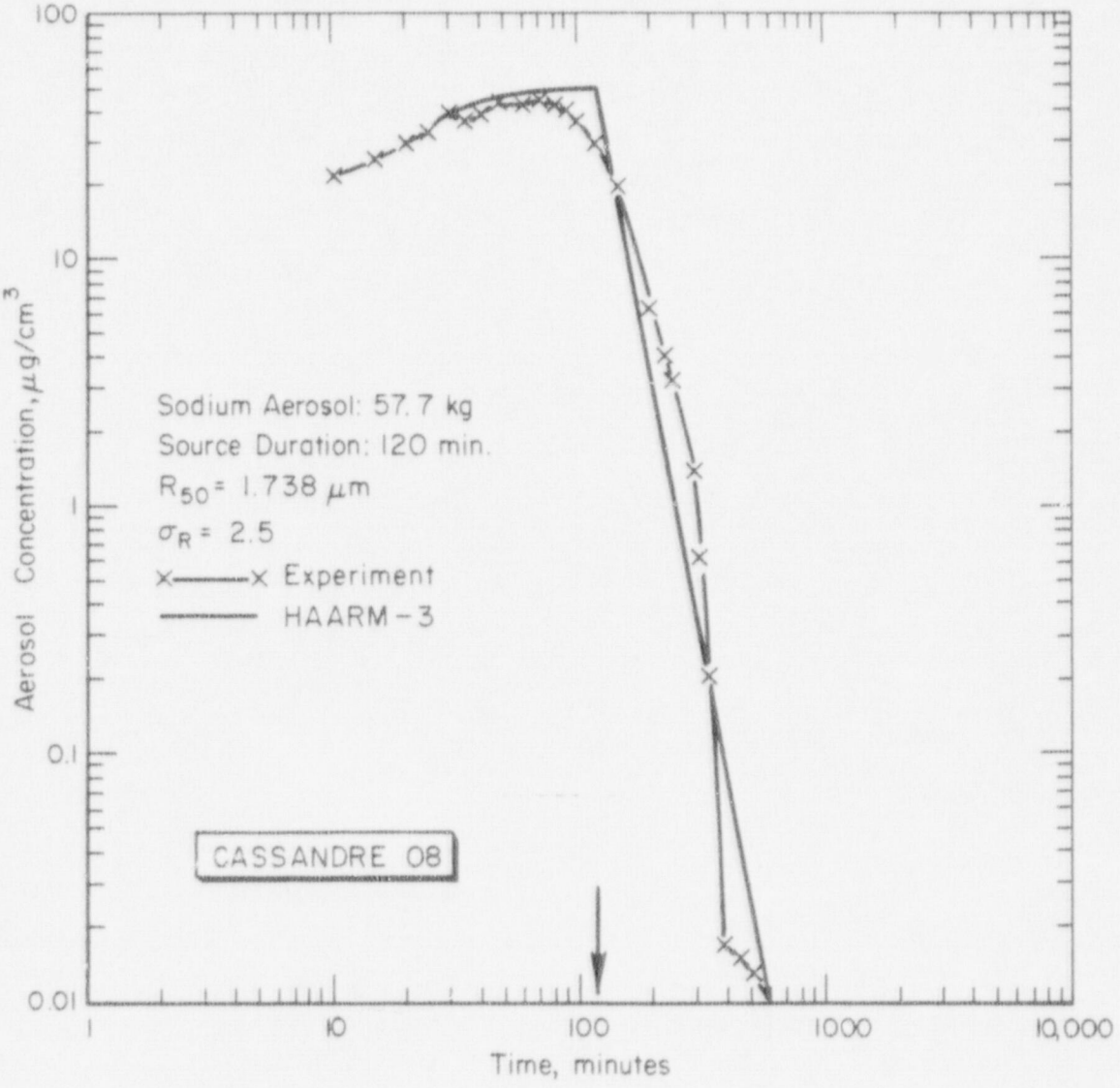

FIGURE 6. COMPARISON OF HAARM-3 CALCULATIONS WITH EXPERIMENTAL DATA -- CASSANDRE TEST 08

EXPERIMENTS TO CHARACTERIZE FUEL MATERIAL-COOLANT AEROSOL PROPERTIES

During this quarter, experiments on the characterization of aerosols formed under various hypothetical LMFBR accident conditions were continued. In order to cover the range of possible aerosol creation environments of a core disruptive accident, the following characteristic conditions are to be investigated:

(1) Fuel vapor condensing to pure fuel aerosol particles in an atmosphere of noble gas fission products

(2) Fuel and cladding/structural material vapors condensing in an atmosphere of noble gas fission products

(3) Fuel vapor condensing in an atmosphere of noble gases and sodium vapor

(4) Fuel cladding/structural material vapors condensing in an atmosphere of noble gases and sodium vapor

(5) Fuel vapor condensing in an atmosphere of pure sodium vapor

(6) Fuel vapor and cladding/structural material vapors condensing in an atmosphere of pure sodium vapor.

Difficulties with the vaporization cell built to produce these conditions were described in the previous quarterly report. Further investigations during this quarter led to development of a completely new vaporization cell design making use of laser induced vaporization. The latter can be expected to circumvent the apparent problems of TaC contamination of the UO_2 vapor that were encountered under some conditions in the previous vaporization cell.

The contamination problem was not completely resolved. While micro-probe analysis of individual particles captured on Millipore filters revealed significant Ta contamination, integral fluorometric examinations of heavily loaded Millipore filters showed little, if any, contamination

when UO_2 was vaporized in an optimal fashion, that is, vaporized at minimum filament temperatures. Higher temperatures did result in measurable Ta contamination by the fluorometric technique.

In order to implement the laser vaporization technique, use will be made of a CO_2 infrared laser available at Battelle. The necessary windows (Kodak IRTRAN-2) were ordered and detailed design of the vaporizer begun.

In order to complete the data base for measurement of the drag correction factor of UO_2 particles, a simple vaporizer using the TaC filament vaporization technique was constructed. To avoid the previously mentioned TaC contamination problem, the vaporization process was carried out at minimum filament temperatures that gave satisfactory UO_2 vaporization. A schematic of this cell is shown in Figure 7. Without the constraint of high temperature capability that was placed on the previous cell, this cell could be made large enough to minimize thermal deposition during the aerosol creation process. The electrodes could also be designed to interface as little as possible. Numerous windows permit easy viewing. Preliminary runs indicated that aerosol could be consistently created and detected, both in the Millikan cell and on filters. Control of creation conditions is achieved visually, that is, current through the filament is regulated to achieve a just visible, minimal but steady particle plume above the UO_2 melt. This technique was adopted in favor of previous methods using pyrometry to determine repeatable creation conditions. The latter were found less reliable due to uneven coating of the filament and consequent wide variations in radiative emissions.

In preparation for experiments on mixed sodium-UO_2 aerosols, the possibility of vaporizing sodium just below the filament by induction heating of a crucible, was investigated using the interim vaporizer. The arrangement of crucible and induction coil relative to the filament does indeed produce copious amounts of sodium aerosol in nitrogen atmospheres. The sodium aerosol could be oxidized successfully by mixing with air in an on-line conditioning chamber.

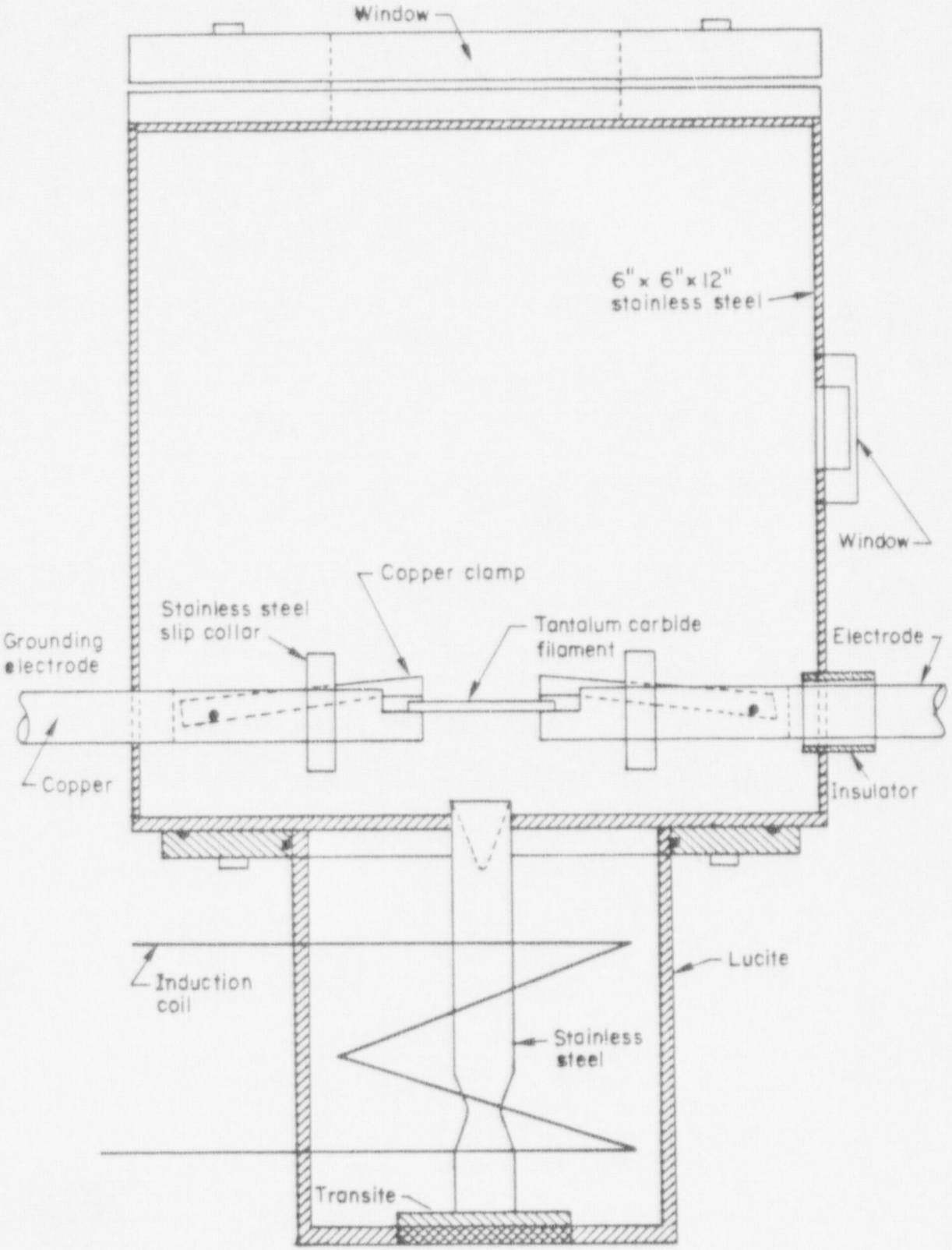

FIGURE 7. SCHEMATIC OF INTERIM UO_2-Na VAPORIZATION CELL

Experiments of Humidity Effects on Sodium Aerosol Formation

Knowledge of aerosol formation characteristics is of importance for accurate predictions of aerosol population behavior. Previously, the shape and density characteristics of sodium oxide agglomerates were studied experimentally[4]. It was found that the shape of sodium oxide agglomerates is strongly dependent on the number of primary particles forming the agglomerate. It was also suggested in the study that the small amount of moisture present in air can greatly affect the characteristics of sodium oxide aerosol formation. As a followup of that study, moisture effects on the particle formation have been examined qualitatively.

The experimental setup used for examining sodium oxide particles under various relative humidity conditions is shown in Figure 8. Compressed air is initially passed through charcoal and ascarite filters, (a) and (b), to remove carbon dioxide and other gases. To achieve a dry condition, the air is subsequently passed through the silica gel and dry ice bath designated by (c) and (d) in the figure. When a nearly 100 percent relative humidity is desired, the air bypasses the above path. Instead, the air is nearly saturated with moisture by passing through the humidifier (e) which is filled with hot water and glass beads. Intermediate humidities can be achieved by appropriately controlling the flow rates through these two paths. The air treated as above is then filtered by an absolute filter (f) to remove any background particles. The actual humidities of the air were then measured by a hygrometer (g).

Using air treated this way, sodium was burned in the combustion chamber (h), and the aerosol produced in the chamber was then directed into an aerosol sampler (i). The sampler used here operates on the principle of thermal precipitation of particles onto an electronmicroscope grid. The details on the design and operation of the combustion chamber and the sampler were described in a previous report[4]. After sampling the aerosol, the sampler was then placed in a plastic gloved bag which was attached to the electronmicroscope and filled with dry air. This procedure was necessary to avoid any possible moisture interference effects by the laboratory air.

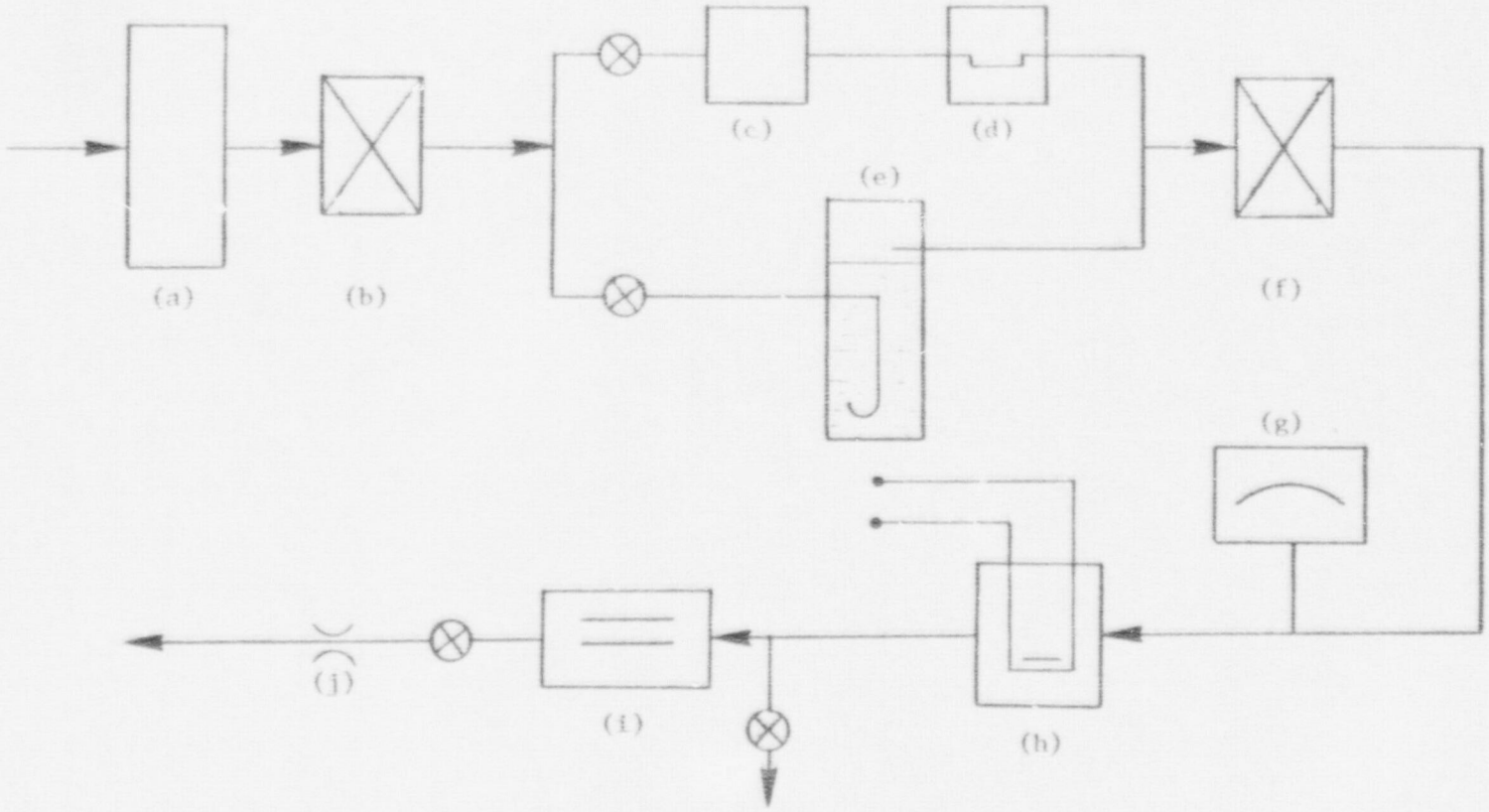

(a) Charcoal Filter; (b) Ascarite Filter; (c) Silica Gel; (d) Dry Ice Bath; (e) Humidifier
(f) Absolute Filter; (g) Hygrometer; (h) Combustion Chamber; (i) Aerosol Sampler; (j) Flow Meter

FIGURE 8. SCHEMATIC DIAGRAM OF THE EXPERIMENTAL SETUP

Figure 9, (a) and (b), show the electron micrographs of the sodium oxide particles generated with the air under the 90 percent relative humdiity condition. It is seen from Figure 9(a) that the particles appear to have contained traces of water or water vapor which evaporated in the microscope. Thus, the overall structure seems to be rather porous. In Figure 9(b), the same kind of particle structure is also observed. However, some particles have a hollow structure and the material of this structure appears to be more solid than the "shell" shape particles. With air of 50 percent relative humidity, the particles in Figure 9(c) and (d) are again seen to have a hollow structure. Figure 10, (a), (b), and (c), show the sodium oxide generated with the air having relative humidities of 30, 15, and 10 percent, respectively. Particles are seen to attain more solid structure as the relative humidity decreases. When the humidity was further reduced such that almost no water vapor was present in the air, the sodium oxide particles as shown in Figure 10(d) were obtained, which have a definite crystal structure. It should be noted that this type of structure was also observed previously[4] when the sodium oxide particles were formed and sampled in completely dry air during analyses of primary particle size distribution.

It is generally known that sodium is extremely reactive even with minute amounts of moisture present in air. According to the vapor-phase reaction mechanisms, sodium can react to form NaO_2 when no moisture is available. Subsequently, NaO_2 can also react with additional sodium and condense on available surface to form Na_2O_2. When a small amount of water is present, however, these reactions become complicated. The sodium can react directly with water vapor to form NaOH and probably Na_2O as a secondary reaction. In addition, the initially formed Na_2O_2 can be converted into a series of hydrates upon reacting with water. Among these, $Na_2O_2 \cdot 8H_2O$ is considered stable and, therefore, may be present if enough water is available. At elevated temperatures, $Na_2O_2 \cdot 8H_2O$ may also react with its own water to form NaOH and release oxygen and water. However, the exact kinetics of these processes and the required conditions such as temperature are not well known for the sodium burning method.

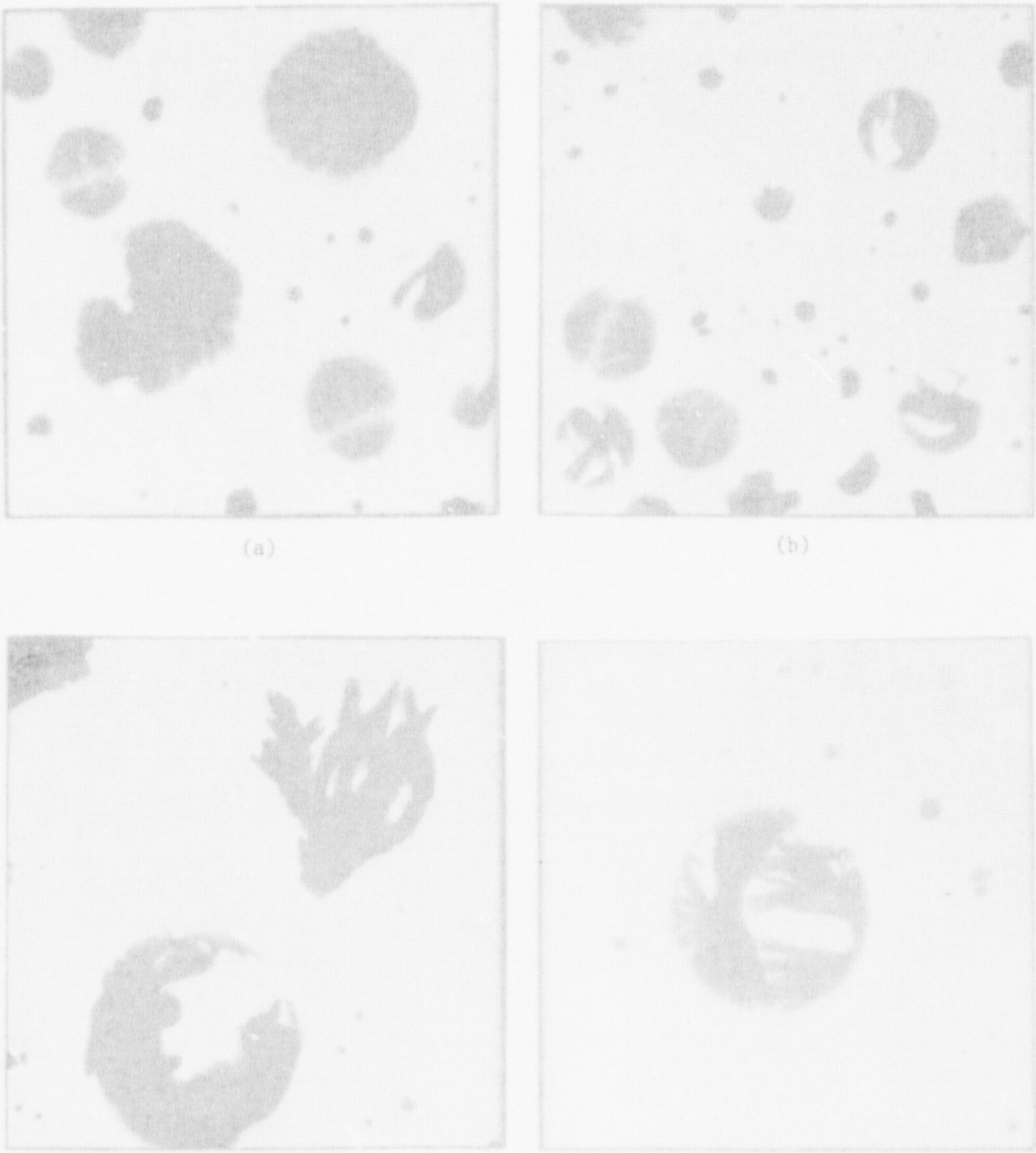

(a) (b)

(c) (d)

FIGURE 9. ELECTRON MICROGRAPHS OF SODIUM OXIDE PARTICLES GENERATED WITH AIR HAVING RELATIVE HUMIDITY OF 90 PERCENT (a,b) AND 50 PERCENT (c,d)

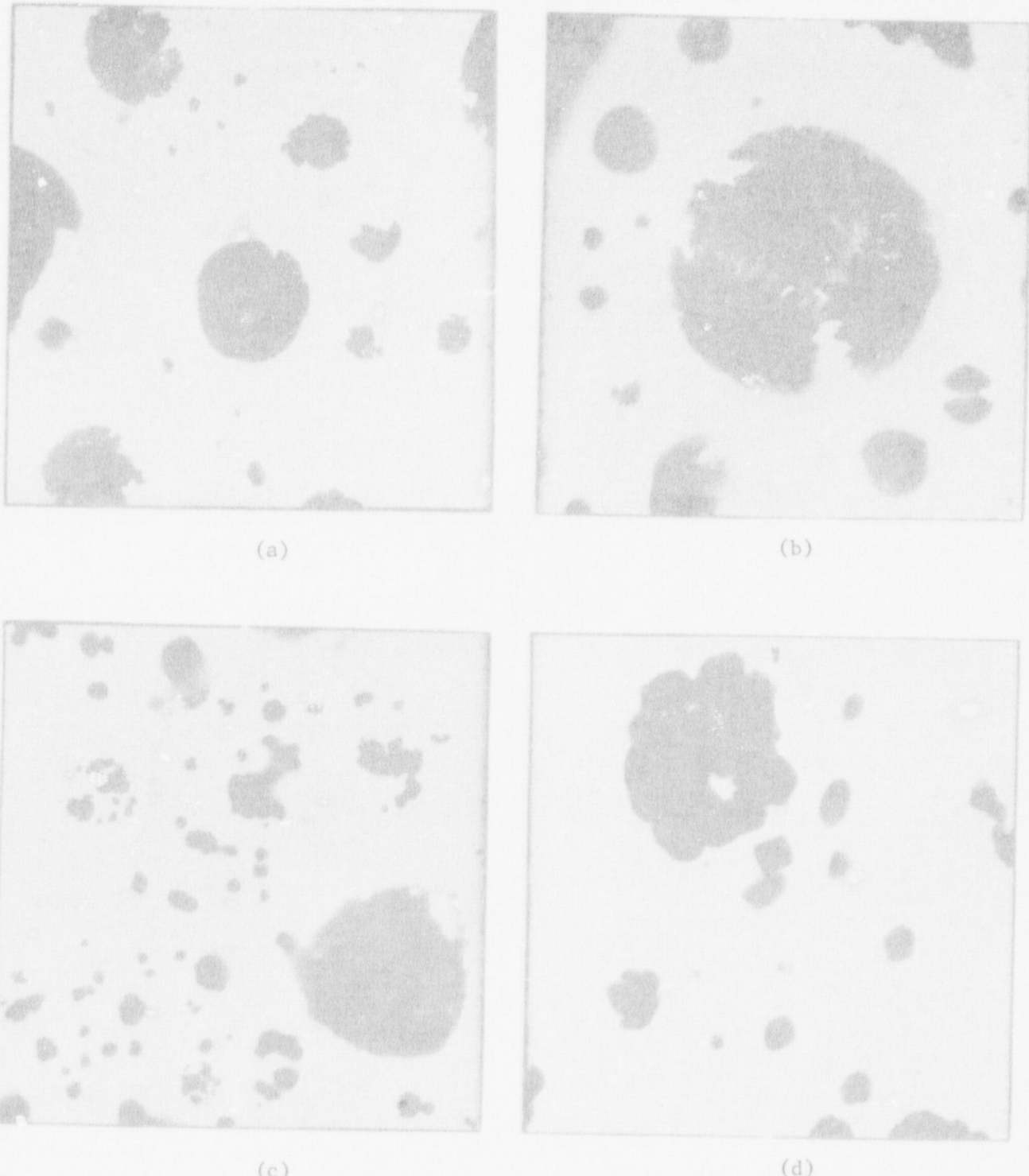

(a) (b)

(c) (d)

FIGURE 10. ELECTRON MICROGRAPHS OF SODIUM OXIDE PARTICLES GENERATED WITH AIR HAVING RELATIVE HUMIDITY OF 30 (a), 15 (b), 10 (c), and 0 (d) PERCENTS

Moreover, relative amounts of these species which may comprise aerosol particles and their spatial distribution relative to sodium fire are very difficult to predict quantitatively.

Some qualitative explanations concerning the aerosol formation, however, can be made in connection with results of the present experiments as follows. In the sodium vapor region of the flame, sodium may react with water such that

$$Na_{(\ell)} + H_2O_{(g)} \rightarrow NaOH_{(s)} + \frac{1}{2} H_{2\,(g)} \quad . \qquad (1)$$

Additionally, the following secondary reaction can take place:

$$Na_{(\ell)} + NaOH_{(s)} \rightarrow Na_2O_{(s)} + \frac{1}{2} H_{2\,(g)} \quad . \qquad (2)$$

When there is enough moisture, Na_2O, which might have been initially formed, may become $Na_2O_2 \cdot 8H_2O$ and then by reacting with its own water component, this can become NaOH, so that

$$Na_2O_2 \cdot 8H_2O \rightarrow 2NaOH_{(s)} + \frac{1}{2} O_{2\,(g)} + 7H_2O_{(\ell)} \quad . \qquad (3)$$

It should be noted that the products of these reactions consist of solids, liquids, and gases (s, ℓ, and g). Thus, it is expected that some of the aerosol formed in this way would have porous structure and hollow, gas-filled particles. It is also probable that some particles are in the form of liquid containing water. Although the present experiments were conducted under different humidity conditions, it is also expected that the samples taken would more or less have some amount of each product.

In summary, results of the present experiments show that sodium and sodium oxide can react with small amounts of water forming a porous or hollow structure. Even at a relative humidity of 10 percent, some of the aerosol particles appear to be either wet or porous. Since particle density, shape and size have all pronounced effects on various aerosol behavior mechanisms, it might be necessary to study further the effects of the presence of various products on the aerosol behavior mechanisms. Until this question is fully answered, it is necessary to be aware of this potential problem and to carefully maintain the moisture at a desired level in large-scale experiments.

DEVELOPMENT OF THE REFERENCE CODE

The problem of continuous formation of increasingly large particles, as coagulation proceeds in time, which exceed the practical limits of maximum sizes set up in any reasonably fast computational scheme, and the consequent lack of mass conservation, led to a close examination of Tolfo's work[5]. It appeared that his approach, which involves a fixed number of size classes and resembles a Lagrangian description of particle behavior, led inherently to conservation of particle mass. Tolfo develops a model of coagulation, based on earlier work of Sutugin and Fuchs[6], in which conservation of mass leads to the following system of 2N simultaneous equations:

$$\frac{d\hat{N}_i}{dt} + \sum_{j<i} K_{ij}\hat{N}_i\hat{N}_j + \frac{1}{2} K_{ii}\hat{N}_i^2 = 0, \qquad i = 1, 2, \ldots N \tag{4a}$$

$$\frac{dx_i}{dt} - \sum_{j<i} K_{ij}\hat{N}_j x_j - \frac{1}{2} K_{ii}\hat{N}_i x_i = 0, \qquad i = 1, 2, \ldots N . \tag{4b}$$

$\hat{N}_i$ is the number of particles in size class i, x_i is the average mass of a particle in size class i, K_{ij} denotes the frequency of collision between particles of classes i and j. It is postulated in deriving Equations (4) that if $x_i > x_j$, then the mass x_j will be added to the total mass of class i; and, if $x_i < x_j$, then the mass x_i will be removed from the total mass of class i. If $x_i = x_j$, it is assumed that half the collisions contribute to increasing the average mass x_i of class i and the other half represent removal of mass from class i.

Tolfo solves the system of Equations (4), assuming that the coefficients in these equations are independent of time for a sufficiently small interval of integration or time increment Δt. The solution to this system is as follows:

$$\hat{N}_N(t) = \left(\frac{1}{2} K_{NN} \cdot \Delta t + [\hat{N}_N(t_o)]^{-1}\right)^{-1} \tag{5a}$$

$$\hat{N}_i(t) = \frac{\beta}{\alpha} \cdot \left| \frac{1}{\left(1 + \frac{\beta}{\alpha \hat{N}_i(t_o)}\right) e^{\beta \cdot \Delta t} - 1} \right| \; ; \qquad i = 1, 2, \ldots N-1 \qquad (5b)$$

$$x_i(t) = -\frac{b}{a} + \left(\frac{a x_i(t_o) + b}{a}\right) e^{-a \cdot \Delta t} \; ; \qquad i = 1, 2, \ldots N \; . \qquad (5c)$$

In Equations (2), $\Delta t = t - t_o$, and

$$\alpha = \frac{1}{2} K_{ii}$$

$$\beta = \left(K_{i,i+1} \hat{N}_{i+1} + K_{i,i+2} \hat{N}_{i+2} + \ldots + K_{iN} \hat{N}_N\right) \qquad (6a)$$

$$a = \frac{1}{2} K_{ii} \hat{N}_i$$

$$b = -\left(K_{1,i} \hat{N}_1 x_1 + K_{2,i} \hat{N}_2 x_2 + \ldots + K_{i-1,i} \hat{N}_{i-1} x_{i-1}\right) . \qquad (6b)$$

Equation (5a) is evaluated first, followed by (5b) for i = N-1, N-2, . . . 2,1, in that order, and finally (5c), in which the values obtained from (5a) and (5b) are used to evaluate the coefficients in (6b).

Tolfo concludes that his model approximates the exact coagulation model reasonably well for small values of the collision frequency K_{ij}, for small coagulation times t, and when the initial number density is highly polydispersed. The population of the intermediate size classes is more abundant in his model in comparison with the exact model, while the opposite is true for the population of the larger size classes. This effect becomes more pronounced as the coagulation time t becomes larger and as the initial number density tends toward a monodispersed distribution.

The Tolfo model was tested for the case of constant kernel ($K_{ij} = 1$), with N = 80, $\Delta x = 0.25$, $\Delta t = 0.05$. The results deviated very greatly from the exact solution of Scott.[7] Also, conservation of particle mass was poor, although the model is supposed to conserve mass by virtue of the basic algorithms. The computational times were also large. It was concluded that, for our purposes, the Tolfo model was very unsatisfactory.

A complete Lagrangian specification of particle behavior during coagulation would be very useful from the standpoint of mass conservation. The evolution in time of the Lagrangian particle mass and the corresponding number distribution in a given 'tagged' size class or channel would be investigated. The number of size classes selected for the initial number distribution would remain unchanged, as the time history of a size class would be followed. This approach is very powerful, but the resulting system of equations is much more complex than the coagulation equation that is being currently investigated. It is, therefore, felt that, under the constraints of this project, it would not be desirable to pursue the Lagrangian approach any further at this time.

The discrete form of the coagulation equation, namely

$$\frac{d\hat{N}_i}{dt} = \frac{1}{2} \sum_{j+\ell=i} K(x_j, x_\ell)\hat{N}_j(t)\hat{N}_\ell(t) - \hat{N}_i(t) \sum_{j=1}^{N} K(x_i, x_j)\hat{N}_j(t) \quad , \tag{7}$$

was solved using Euler integration, in order to compare the accuracy of solutions and computational speed with the Tolfo model. The Scott and Golovin[8] cases were run for $\Delta x = 0.25$, $N = 80$, and $t = 2.0$. In both cases, the numerical solution of (7) matched the analytic results closely. Also, the speed of computation was much greater than that obtained with the Tolfo model.

Equation (7) was also solved for the initial condition of a histogram approximation to the lognormal distribution and constant kernel. The same initial distribution was spanned by 7 mass classes in one case and by 14 mass classes in another case, and the total number of mass classes, N, was 80 in each case. The objective was to determine the effect of resolution of the initial distribution on the number distribution. That is, the resolution required of the initial distribution determines the mass class increments and therefore the maximum mass class that can be considered given a fixed number of mass classes. The results are shown in Figure 11. It is seen that the results are not very sensitive to differences in the resolution of the initial distribution. However, further work is needed before more definitive conclusions can be made.

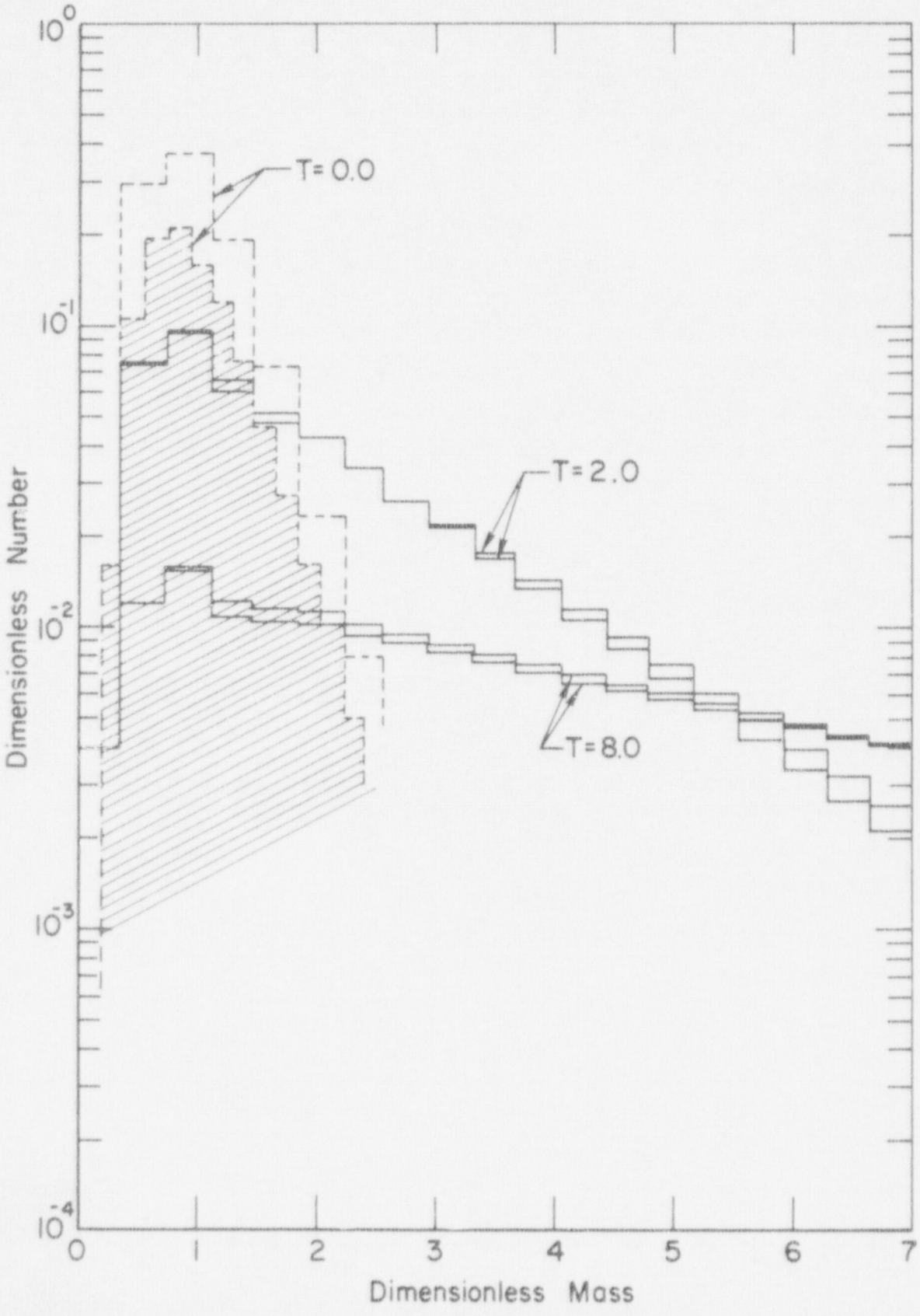

FIGURE 11. THE EFFECT OF THE RESOLUTION OF THE INITIAL DISTRIBUTION ON THE NUMBER DISTRIBUTION

It was felt that in order to improve conservation of particle mass for certain types of kernels, such as that used by Golovin, a larger number of size classes N would be required. Thus far, the reference code uses two N x N matrices, which are difficult to store in the Battelle computer for large values of N. It was, therefore, decided to try another method of solving the equations for the number distribution, namely the method of solving tridiagonal linear systems of equations. This method was comparable in accuracy and computation time to the earlier method used for the Golovin case, with $\Delta x = 0.5$, $N = 80$, and $t=2.0$. However, in using this method, it was not possible to choose a reasonable criterion for selecting the time step, as the variables used in this method could not be interpreted physically. This method was, therefore, regarded as inadequate for the purposes of the reference code. It was thus considered necessary to seek more satisfactory approaches toward the numerical solution of the coagulation equation.

REFERENCES

(1) Permandjian, J., "Comportement des Aerosols Sodes Dans Une Enceinte Confinee. Interpretation des Essais Cassandre au Moyen des Codes de Calcul Pardiseko 3 et Haarm 2", Rapport Setssr No. 65, Commissariat a L'Energie Atomique, 41 (September, 1977).

(2) Adams, R. E., Kress, T. S. and Parsly, L. F., Jr., "Sodium Oxide Aerosol Study: NSPP Runs 101-105, Data Record Report", Oak Ridge National Laboratory ORNL/NUREG/TM-179.

(3) Gieseke, J. A., Jordan H., Lee, K. W., Vaishnavi, B., and Reed, L. D., "Aerosol Measurements and Modeling for Fast Breeder [illegible]or Safety: Annual Report for FY 1977", BMI-NUREG-1989, Batte[illegible]mbus (December, 1977).

(4) Gieseke, J. A., Reed, L. D., Jordan, H., and Lee [illegible]W., "Characteristics of Agglomerates of Sodium Oxide Aerosol Particles. [illegible]opical Report", BMI-NUREG-1977, Battelle-Columbus (August, 1977).

(5) Tolfo, F. "A Simplified Model of Aerosol Coagulation", J. Aerosol Sci., 8, 9-19 (1977).

(6) Sutugin, A. G., and Fuchs, N. A., "Formation of Condensation Aerosols at High Vapor Supersaturation," J. Colloid and Interface Sci., 27 (2), 216-228 (1968).

(7) Scott, W. T., "Analytic Studies of Cloud Droplet Coalescence I", J. of Atmos. Sci., 25, 54-65 (1968).

(8) Golovin, A. M., "The Solution of the Coagulation Equation for Cloud Droplets in a Rising Air Current", Bull. Acad. of Sci., USSR, Geophys. Ser. (English Ed.), No. 5 (1963).

DISTRIBUTION LIST

310 copies -- Distribution under R7

Supplemental Distribution

Dr. James A. Gieseke (15)
Research Leader
Battelle, Columbus Laboratories
505 King Avenue
Columbus, Ohio 43201

Prof. David T. Shaw (1)
Department of Engineering Science
Aerospace Engineering and Nuclear Engineering
State University of New York at Buffalo
4232 Ridge Lea Road
Buffalo, New York 14226

Dr. Harry A. Morewitz, Manager (1)
LMFBR Physics and Safety
Atomics International Division
Rockwell International
8900 DeSoto Avenue
Canoga Park, California 91304

Dr. S. K. Loyalka (1)
Associate Professor
Nuclear Engineering
1026 Engineering
University of Missouri
Columbia Missouri 65201

NRC FORM 335 (7-77)

U.S. NUCLEAR REGULATORY COMMISSION

BIBLIOGRAPHIC DATA SHEET

1. REPORT NUMBER (Assigned by DDC)
NUREG/CR-0425
BMI-2005

4. TITLE AND SUBTITLE (Add Volume No., if appropriate)
AEROSOL MEASUREMENTS AND MODELING FOR TAST REACTOR SAFETY - QUARTERLY PROGRESS REPORT - JANUARY THROUGH MARCH 1978

2. (Leave blank)

3. RECIPIENT'S ACCESSION NO.

7. AUTHOR(S)
J.A. Gieseke and others

5. DATE REPORT COMPLETED
MONTH: September YEAR: 1978

9. PERFORMING ORGANIZATION NAME AND MAILING ADDRESS (Include Zip Code)
Battelle-Columbus Laboratory
505 King Avenue
Columbus, Ohio 43201

DATE REPORT ISSUED
MONTH: October YEAR: 1978

6. (Leave blank)

8. (Leave blank)

12. SPONSORING ORGANIZATION NAME AND MAILING ADDRESS (Include Zip Code)
Division of Reactor Safety Research
Office of Nuclear Regulatory Research
U.S. Nuclear Regulatory Commission

10. PROJECT/TASK/WORK UNIT NO.

11. CONTRACT NO.
NRC-04-76-293-07

13. TYPE OF REPORT
Quarterly Progress Report

PERIOD COVERED (Inclusive dates)
January - March 1978

15. SUPPLEMENTARY NOTES

14. (Leave blank)

16. ABSTRACT (200 words or less)

Technical progress during this quarter was made on the comparison of the HAARM-3 computer code with aerosol measurements, experimental measurements of uranium oxide aerosol characteristics, determinations of humidity effects on sodium aerosol formation, and development of the reference code. In addition, a mid-year review was presented to NRC staff on February 16, 1978. Technical progress on each of the above topics is discussed in this report.

17. KEY WORDS AND DOCUMENT ANALYSIS

17a. DESCRIPTORS

17b. IDENTIFIERS/OPEN-ENDED TERMS

18. AVAILABILITY STATEMENT
Unlimited

19. SECURITY CLASS (This report)

21. NO. OF PAGES

20. SECURITY CLASS (This page)

22. PRICE
$